

**DOKUZ EYLÜL UNIVERSITY**  
**GRADUATE SCHOOL OF NATURAL AND APPLIED**  
**SCIENCES**

**DETERMINATION OF QUALITATIVE AND**  
**QUANTITATIVE PROPERTIES OF NATURAL**  
**STONES USING SIGNAL AND IMAGE**  
**PROCESSING TECHNIQUES**

**by**  
**Osman Tayfun BİŞKİN**

**July, 2011**

**İZMİR**

**DETERMINATION OF QUALITATIVE AND  
QUANTITATIVE PROPERTIES OF NATURAL  
STONES USING SIGNAL AND IMAGE  
PROCESSING TECHNIQUES**

**A Thesis Submitted to the  
Graduate School of Natural and Applied Sciences of Dokuz Eylül University  
In Partial Fulfillment of the Requirements for the Degree of Master of Science  
in Electrical and Electronics Engineering**

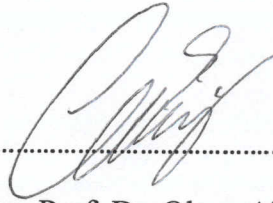
**by  
Osman Tayfun BİŞKİN**

**July, 2011**

**İZMİR**

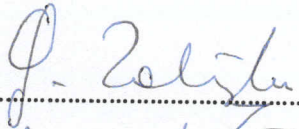
## M.Sc THESIS EXAMINATION RESULT FORM

We have read the thesis entitled “**DETERMINATION OF QUALITATIVE AND QUANTITATIVE PROPERTIES OF NATURAL STONES BY USING SIGNAL AND IMAGE PROCESSING TECHNIQUES**” completed by **OSMAN TAYFUN BİŞKİN** under supervision of **ASSOC. PROF. DR. OLCAY AKAY** and we certify that in our opinion it is fully adequate, in scope and in quality, as a thesis for the degree of Master of Science.



Assoc. Prof. Dr. Olcay AKAY

Supervisor



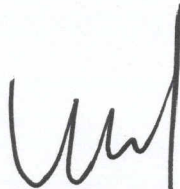
Prof. Dr. G. Zekiye

(Jury Member)



Asst. Prof. Dr. Okan ÖNAL

(Jury Member)



Prof. Dr. Mustafa SABUNCU

Director

Graduate School of Natural and Applied Sciences

## **ACKNOWLEDGMENTS**

First of all, I would like to thank my advisor Assoc. Prof. Dr. Olcay AKAY for his patient support and valuable guidance during this thesis study. I must express that his encouragement, polite attitude and new ideas made this work possible. I also would like to thank Asst. Prof. Dr. M. Alper SELVER for his support and encouragement. His new ideas and work discipline always motivated me.

I also would like to thank TURKCELL for its support throughout my master degree.

Finally, I thank my family, the meaning of my life, for their never-ending support throughout my life.

Osman Tayfun BİŞKİN



# **DETERMINATION OF QUALITATIVE AND QUANTITATIVE PROPERTIES OF NATURAL STONES USING SIGNAL AND IMAGE PROCESSING TECHNIQUES**

## **ABSTRACT**

Marble is a member of the large community of natural stones. It is used in structures for decorative and other purposes extensively. Use of marble in building sector gives it an economical importance. Quality of a marble is a main attribute that affects its cost. Therefore, determination of qualitative and quantitative properties of marbles is of interest. Strength of a marble can be characterized by means of uniaxial compressive strength (UCS). This parameter can be determined by destructive laboratory testing methods. After being subject to destructive testing, marbles cannot be used anymore. Therefore, our aim is to determine UCS by using nondestructive methods. In this thesis, instead of using destructive tests, nondestructive laboratory testing methods are employed together with various signal and image processing techniques in order to determine UCS values of cubic marble samples. Performances of different features obtained using signal and image processing techniques and nondestructive laboratory testing methods are compared via simulation results. A feature selection method is also applied in order to decrease the number of features and to increase the prediction success of UCS values. Success of prediction of UCS values (with and without feature selection) is compared and correlations between selected features and UCS values are investigated. Simulations are accomplished with different types of learning methods. Random sub-sampling, K-fold cross-validation, leave-one-out cross-validation, and bootstrap learning methods are used during training of multilayered perceptron (MLP) neural networks.

**Keywords:** Prediction of uniaxial compressive strength, feature selection, sum and difference histograms, learning methods, multilayered perceptron (MLP) neural networks.

# DOĞAL TAŞLARIN NİCEL VE NİTEL ÖZELLİKLERİNİN SİNYAL VE GÖRÜNTÜ İŞLEME TEKNİKLERİ KULLANILARAK BELİRLENMESİ

## ÖZ

Mermer doğal taşlar ailesinin bir üyesidir. Mermerler günlük hayatta yapılarda, dekorasyon malzemelerinde ve diğer amaçlarla yoğun olarak kullanılırlar. Mermerlerin inşaat sektöründe kullanılmaları ekonomik önem kazanmalarını sağlamıştır. Bir mermerin kalitesi onun maliyetini etkileyen ana özelliktir. Bundan dolayı, mermerlerin nitel ve nicel özelliklerinin belirlenmesi önemlidir. Bir mermerin dayanıklılığı tek eksenli basınç dayanım değerine göre nitelendirilir. Bu değer tahribatlı laboratuvar testleri ile elde edilir ve yıkıcı olan bu laboratuvar testleri sonunda mermer artık bir daha kullanılamaz hale gelir. Bu nedenden dolayı, amacımız tek eksenli basınç dayanım değerlerinin yıkıcı olmayan metotlarla belirlenmesidir. Bu tezde, mermer küp örneklerin tek eksenli basınç dayanım değerlerini tahmin etmek için yıkıcı test metotlarını kullanmak yerine, tahribatsız laboratuvar testleri sinyal ve görüntü işleme teknikleri ile birlikte kullanıldı. Sinyal ve görüntü işleme tekniklerinden ve yıkıcı olmayan laboratuvar testlerinden elde edilen farklı özneteliklerin başarımlı benzetim sonuçları kullanılarak karşılaştırıldı. Öznetelik sayısını düşürmek ve tek eksenli basınç dayanım değerlerinin öngörülme başarısını artırmak için bir öznetelik seçim metodu uygulandı. Tek eksenli basınç dayanım değerlerinin (öznetelik seçimiyle ve öznetelik seçimi olmadan) öngörülmesindeki başarımlar karşılaştırıldı ve seçilen öznetelikler ile tek eksenli basınç dayanım değerleri arasında ilinti araştırıldı. Benzetimler farklı tiplerdeki öğrenim metodları ile gerçekleştirildi. Çok katmanlı algılayıcı yapay sinir ağları eğitilirken, rastgele seyrek örnekleme (Random sub-sampling), K-fold çarpaz-sağlama (K-fold cross-validation), leave-one-out çarpaz-sağlama, önyükleme (bootstrap) öğrenim metodları kullanıldı.

**Anahtar Sözcükler:** Tek eksenli basınç dayanımını öngörme, öznetelik seçimi, toplam ve fark histogramları, öğrenim metodları, Çok Katmanlı Algılayıcı (ÇKA) yapay sinir ağları.

## CONTENTS

	Page
M.Sc THESIS EXAMINATION RESULT FORM .....	ii
ACKNOWLEDGMENTS.....	iii
ABSTRACT .....	iv
ÖZ .....	v
<b>CHAPTER ONE - INTRODUCTION .....</b>	<b>1</b>
1.1 Introduction.....	1
<b>CHAPTER TWO - DATASET.....</b>	<b>4</b>
2.1 Acquisition of Marble Images.....	4
2.2 Image Database and Quality Classes.....	6
<b>CHAPTER THREE - FEATURE EXTRACTION AND SELECTION.....</b>	<b>8</b>
3.1 Sum and Difference Histograms (SDH).....	8
3.1.1 Texture Features Extracted From SDH.....	11
3.2 Wavelet Transform.....	12
3.3 Region Based Features .....	15
3.4 Nondestructive Laboratory Testing.....	17
3.5 Feature Selection .....	19
<b>CHAPTER FOUR - NEURAL NETWORKS AND LEARNING METHODS..</b>	<b>22</b>
4.1 Neural Networks.....	22
4.1.1 Multilayered Perceptrons.....	23

4.2 Learning Methods.....	25
<b>CHAPTER FIVE - SIMULATION RESULTS .....</b>	<b>28</b>
5.1 Determination of UCS Using Sum and Difference Histogram (SDH) Features .....	29
5.2 Determination of UCS Using Wavelet Features .....	31
5.3 Determination of UCS Using Region Based Features.....	34
5.4 Determination of UCS Using Nondestructive Laboratory Testing.....	36
<b>CHAPTER SIX - CONCLUSIONS.....</b>	<b>39</b>
<b>REFERENCES .....</b>	<b>45</b>
<b>LIST OF FIGURES .....</b>	<b>47</b>
<b>LIST OF TABLES .....</b>	<b>48</b>

## CHAPTER ONE

### INTRODUCTION

#### 1.1 Introduction

Marbles are important natural stones that are used in structures mostly for decoration purposes. This gives marbles an economical importance. Quality of marbles is the main attribute that affects their cost. Therefore, determination of qualitative and quantitative properties of marbles becomes an important issue.

In order to determine the marble strength, which is characterized by means of the uniaxial compressive strength (UCS) parameter, destructive laboratory testing (DLT) procedures are used (Figure 1.1). After applying DLT, a marble sample cannot be used anymore. Therefore, nondestructive laboratory testing (NDT) methods are important to prevent loss of time and destruction of marble samples. In addition to NDT data, features obtained by signal and image processing techniques can also be used to determine UCS.



Figure 1.1 Destructive laboratory testing to determine UCS (TÜBİTAK MAG 104M358).

In the literature, there are a limited number of studies about determination of axial strength of marbles. These works state that the strength of natural stones can be characterized by means of UCS and some correlation can be established between UCS and other rock characteristics (Gokceoglu, 2002; Selver, Ardali, Onal, & Akay, 2008; Sonmez, Tuncay, & Gokceoglu, 2004). This thesis is a follow-up to the work (Selver, et al., 2008) with the aim of improving the performance of methods proposed and studied in that work, and furthermore, to propose new methods. As an extension to the nondestructive laboratory test results used in that study, we extract new features by using signal and image processing techniques. Results obtained in this thesis are also compared with the results of (Selver, et al., 2008).

In this thesis, the same dataset, which was also used in studies (Ardali, 2008; Selver, et al., 2008), is used. Therefore, the background information in Chapter 2 is mostly borrowed from (Ardali, 2008). In Chapter 2, the dataset is introduced. Acquisition of marble sample images is explained in that chapter. Quality groups of marble samples are also described.

Extracted features are explained in Chapter 3. These features are obtained by using sum and difference histograms, wavelet analysis, nondestructive laboratory tests, and by using regional properties of marble surface images. A feature selection method, which is used to reduce the dimensionality of data and to increase the performance of determination of axial strengths of marbles, is also explained in Chapter 3.

Neural networks are introduced briefly in Chapter 4. In addition to neural networks, different learning methods that are used for training of neural networks are also explained in that chapter.

In Chapter 5, simulation results are presented. First of all, extracted features are simulated. Then, a special type of feature selection method is applied. Performance of the system using only the features that are obtained after feature selection is compared with the results obtained without using feature selection. All simulations are performed using multilayered perceptron (MLP) neural networks.

Conclusions and comments on the simulation results are given in Chapter 6. Strengths and weaknesses of the proposed methods are also discussed.

## CHAPTER TWO

### DATASET

In this chapter, the dataset used in this thesis is introduced briefly. Originally, the dataset was collected for the research project TÜBİTAK MAG 104M358 and used to predict the UCS of marbles (Selver, et al., 2008), (Önal, 2008) and for classification of marble surface images (Ardalı, 2008).

#### 2.1 Acquisition of Marble Images

Marble image data were collected at Dokuz Eylül University, Torbalı Vocational School and Civil Engineering Department under the scope of TÜBİTAK MAG 104M358 research project. Marble blocks come from a marble mine near Saruhanlı, Manisa, Turkey. Marble samples are cut in the form of  $7\times7\times7$  cm cubes (Figure 2.1).



Figure 2.1 A polished  $7\times7\times7$  cm cubic marble sample.



In order to prepare a marble sample for image acquisition, each face of the marble cube is polished to give it a better visual appearance. As seen in Figure 2.2, this process increases contrast of marble images.

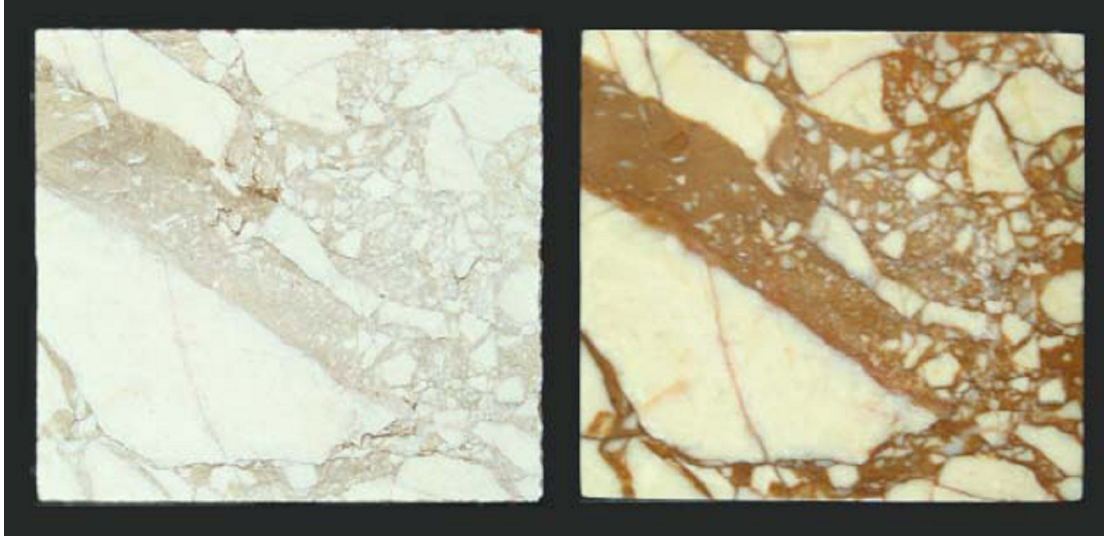


Figure 2.2 Marble block before and after polishing. Visual difference is clear.

Acquisition of images takes place in a  $50 \times 50 \times 80$  cm closed container which is illuminated by fluorescent lamps. Image acquisition system can be seen in Figure 2.3. Marble images are captured at a  $2304 \times 3456$  resolution by using a digital camera. Black background part is removed from images because it is unnecessary for prediction, and thus, images are scaled down to a  $315 \times 310$  resolution level, also reducing computational cost during the simulations.



Figure 2.3 Image acquisition system.

Images of 6 faces of a marble cube are obtained. Each face of this cube is labeled systematically as seen below in Figure 2.4.

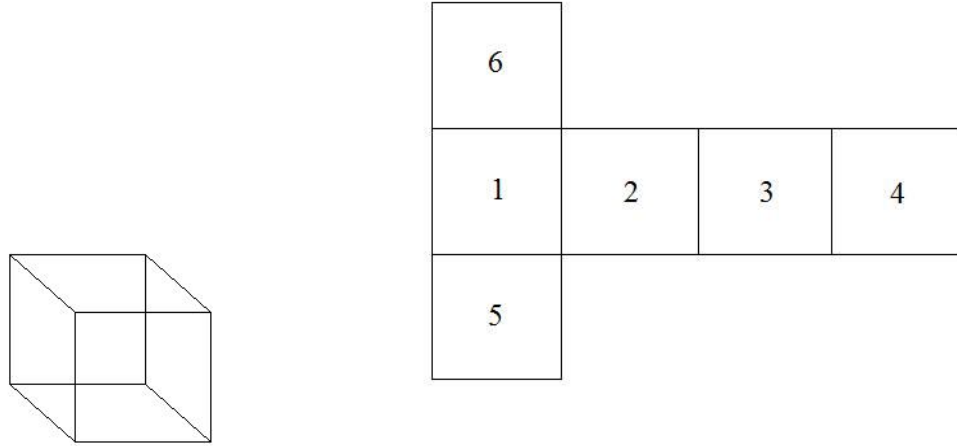


Figure 2.4 Labels of marble surfaces.

## 2.2 Image Database and Quality Classes

After surface images of cubic marble samples are obtained and preprocessed, they are classified into four quality groups by Dokuz Eylül University, Civil Engineering Department experts. These four quality groups may be defined as;

- i) Homogenous limestone (Figure 2.5(a)),
- ii) Limestone with veins (Figure 2.5(b)),
- iii) Fine grains (limestone) separated by cohesive matrix (Figure 2.5(c)),
- iv) Homogenous cohesive matrix (Figure 2.5(d)).

The quality group of a marble sample greatly affects its UCS because UCS values are believed to be correlated to a certain degree with quality groups of marbles. The highest UCS values belong to homogenous limestone samples (Group 1) and the lowest UCS values belong to samples of homogenous cohesive matrix (Group 4). Pictures of typical samples from each quality group are seen in Figure 2.5.

In this thesis, 157 cubic marble samples are used in experiments. Group 1 has 18, Group 2 has 49, Group 3 has 60, and Group 4 has 30 members, respectively.

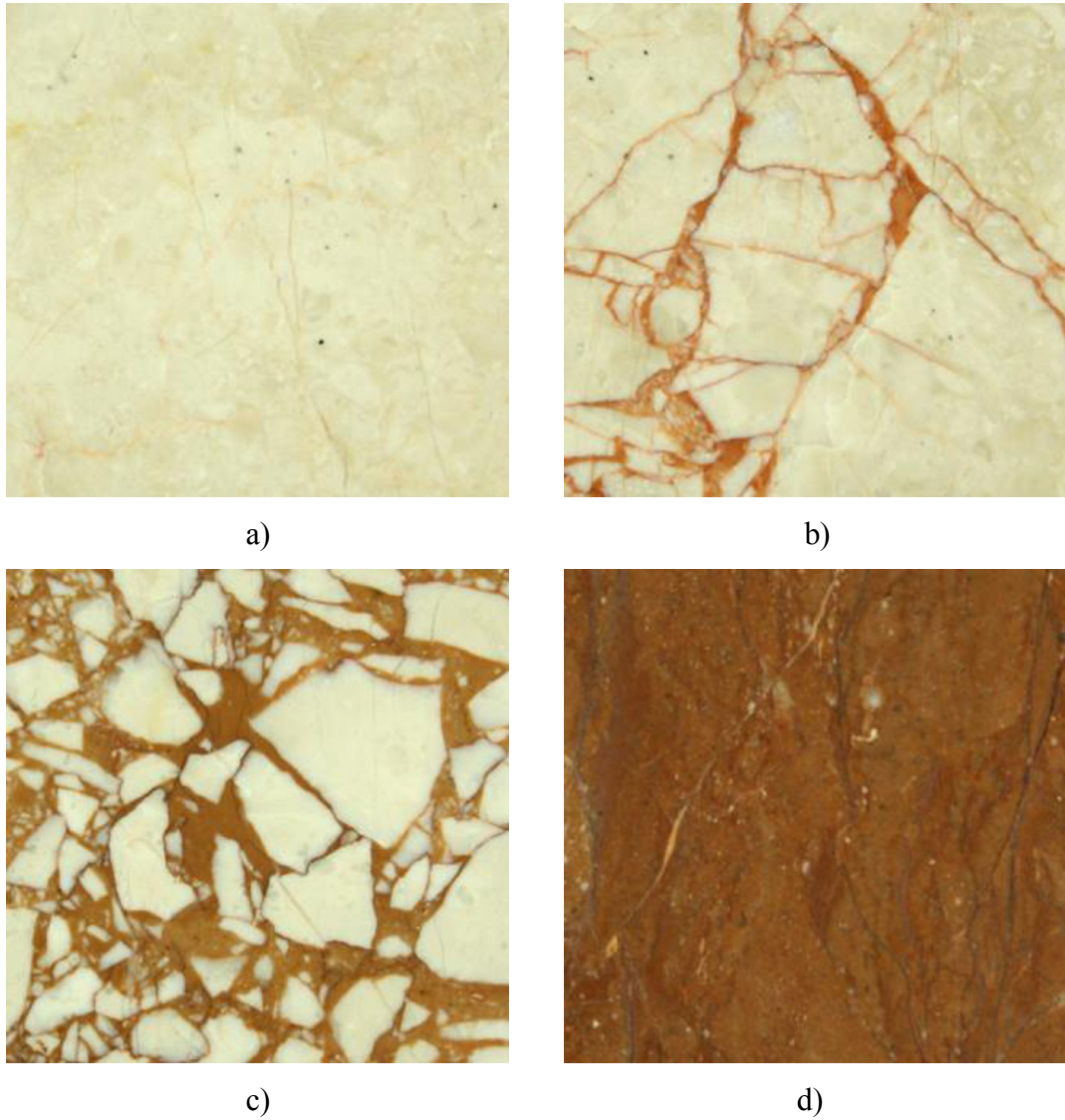


Figure 2.5 Marble images from each quality group; (a) Homogenous limestone, (b) Limestone with veins, (c) Images containing grains separated by cohesive matrix, (d) Homogenous cohesive matrix.

## CHAPTER THREE

### FEATURE EXTRACTION AND SELECTION

In this chapter, different features that are extracted for prediction of UCS are studied. These features are obtained by using sum and difference histograms, wavelet analysis, nondestructive laboratory tests, and by using regional properties of a marble surface image. Finally, a feature selection method is explained. The process of feature selection is employed to reduce the dimension of data and to increase the performance of determination of axial strength of marbles.

#### 3.1 Sum and Difference Histograms (SDH)

Texture is the term used to characterize the surface of a given object or phenomenon (Unser, 1986). Sum and Difference Histograms (SDH) are a useful textural information extraction method first introduced by Unser (Unser, 1986; Ardali, 2008). The sum and difference of two random variables with the same variance are decorrelated and define the principle axes of their associated joint probability function (Unser, 1986). They are based on sum and difference of a pixel with its neighbor pixels. In order to explain the sum and difference histograms method, consider an image with size  $K \times L$ . It can be denoted by  $\{y_{k,l}\}$ ,  $k = 1, 2, \dots, K$ ,  $l = 1, 2, \dots, L$  with grey levels  $G = \{0, 1, \dots, N_G - 1\}$ . Sum and difference are found as

$$\begin{aligned} s_{k,l} &= y_{k,l} + y_{k+d1,l+d2} \\ d_{k,l} &= y_{k,l} - y_{k+d1,l+d2} \end{aligned} \tag{3.1}$$

where  $y_{k,l}$  and  $y_{k+d1,l+d2}$  denote the pixels in the image,  $(d1, d2) \in D$  represent the distances of two pixels, and  $D$  is the subset of indices specifying the texture region to be analyzed. If there are  $N_G$  gray levels,  $1 \times (2N_G - 1)$  dimensional normalized sum and difference histogram vectors can be written as

$$\begin{aligned}
P_s(i) &= h_s(i) / N; & i &= 0, 1, \dots, 2N_G - 2 \\
P_d(j) &= h_d(j) / N; & j &= -N_G + 1, \dots, 0, 1, \dots, N_G - 1
\end{aligned} \tag{3.2}$$

where

$$\begin{aligned}
h_s(i) &= \text{Card}\{(k, l) \in D, s_{k,l} = i\} \\
h_d(j) &= \text{Card}\{(k, l) \in D, d_{k,l} = j\} \\
N &= \text{Card}\{D\} = \sum_i h_s(i) = \sum_j h_d(j)
\end{aligned} \tag{3.3}$$

Card function gives the number of elements in the set that is its argument. Therefore sum and difference histogram vectors can be thought as probability functions. To obtain the SDH, distance set is selected as 8 neighborhoods in this study as in (Ardalı, 2008).

(-1, 1)	(0, 1)	(1, 1)
(-1, 0)	* (0, 0)	(1, 0)
(-1, -1)	(0, -1)	(1, -1)

Figure 3.1 8 pixel neighborhoods for SDH.

In order to explain SDH, two example images and their sum and difference values of neighbor pixels and the center pixel are given below (Ardalı, 2008).

1	1	0
0	0	1
1	0	1

(a)

0	0	0
1	1	0
1	1	1

(b)

Figure 3.2 Two example images.

In Table 3.1,  $s[1]$  and  $s[2]$  represent the sum of the first and second images, respectively.  $d[1]$  and  $d[2]$  represent the difference of the first and second images, respectively. The  $(0,0)$  index in  $s[1]_{0,0}$  and other sum and difference values shows that these values are calculated for a pixel located at  $(0,0)$ . “n” is the neighbor of pixel  $(0,0)$ , for this example.  $(-1,1)$  index in  $n_{(-1,1)}$  indicates pixel  $(-1,1)$  in an image. In Table 3.1 below, rows under the  $n_{(-1,1)}$  shows sum and difference of pixel at  $(0,0)$  and pixel at  $(-1,1)$ .

Table 3.1 Sum and difference values of example images.

	$n_{(-1,1)}$	$n_{(0,1)}$	$n_{(1,1)}$	$n_{(-1,0)}$	$n_{(1,0)}$	$n_{(-1,-1)}$	$n_{(0,-1)}$	$n_{(1,-1)}$
$s[1]_{0,0}$	1	1	0	0	1	1	0	1
$d[1]_{0,0}$	-1	-1	0	0	-1	-1	0	-1
$s[2]_{0,0}$	1	1	1	2	1	2	2	2
$d[2]_{0,0}$	1	1	1	0	1	0	0	0

Normalized sum and difference histograms of these two images can be written using Table 3.1 above as

$$P[1]_s(i) = [0.375 \quad 0.625 \quad 0.000]$$

$$P[1]_d(j) = [0.625 \quad 0.375 \quad 0.000]$$

$$P[2]_s(i) = [0.000 \quad 0.500 \quad 0.500]$$

$$P[2]_d(j) = [0.000 \quad 0.500 \quad 0.500]$$

where  $i = 0, 1, 2$  and  $j = -1, 0, 1$ .  $i$  and  $j$  are the indices of sum histograms and difference histograms, respectively. Therefore, the minimum value of  $i$  is 0 and the maximum value of  $i$  is 2. Similarly, the minimum value of  $j$  is -1 and the maximum value of  $j$  is 1. Thus, these two images have different SDH. Therefore, SDH can be

used to separate these images. However, in order to distinguish images, some features must be extracted from SDH. In this thesis, statistical features which are given in (Unser, 1986) (and which are also used in (Ardalı, 2008)) are used to distinguish marble surface images.

### 3.1.1 Texture Features Extracted From SDH

SDH are used to extract some features from images. In this work, the textural features extracted from SDH are mean, variance, energy, correlation, entropy, contrast, and homogeneity (if there are many gray level transitions, homogeneity will be low). These seven features are defined as stated in (Unser, 1986) and (Ardalı, 2008) and shown in Table 3.2 below.

Table 3.2 Statistical features obtained by SDH.

Features	Formula
Mean	$\mu = \frac{1}{2} \sum_i i P_s(i)$
Variance	$\frac{1}{2} \left( \sum_i (i - 2\mu)^2 P_s(i) + \sum_j j^2 P_d(j) \right)$
Energy	$\sum_i P_s(i)^2 \sum_j P_d(j)^2$
Correlation	$\frac{1}{2} \left( \sum_i (i - 2\mu)^2 P_s(i) - \sum_j j^2 P_d(j) \right)$
Entropy	$-\sum_i P_s(i) \log(P_s(i)) - \sum_j P_d(j) \log(P_d(j))$
Contrast	$\sum_j j^2 P_d(j)$
Homogeneity	$\sum_j \frac{1}{1 + j^2} P_d(j)$

### 3.2 Wavelet Transform

The application of wavelet transform analysis in science and engineering began to take off at the beginning of the 1990s, with a rapid growth in the numbers of researchers turning their attention to wavelet analysis during that decade (Addison, 2002). The wavelet transform is a kind of transformation which facilitates to examine the signal in both time and frequency domains. Functions used in wavelet transform are waves and locations and scales of these waves are different. These functions are named as wavelets. Wavelets are generated from a basic wavelet which is called the mother wavelet. Wavelet functions must have finite energy and zero mean.

In this thesis, wavelet transform is applied to two-dimensional signals, namely images of marble samples. There are some previous works in the literature that use wavelet transform of marble images (Delgado, Alajarin, & Balibrea, 2003; Ardalı, 2008). Digital images of marble sample surfaces are inherently discrete-time signals and hence, the discrete wavelet transform (DWT) is used to extract features. DWT can be expressed as

$$T_{m,n} = \int_{-\infty}^{\infty} x(t)\psi_{m,n}(t)dt \quad (3.4)$$

where  $x(t)$  is the original signal,  $T_{m,n}$  is the wavelet coefficient and  $\psi_{m,n}(t)$  is the orthonormal wavelet basis which can be written as

$$\psi_{m,n}(t) = \frac{1}{\sqrt{a_0^m}} \psi\left(\frac{t - nb_0a_0^m}{a_0^m}\right) \quad (3.5)$$

Here,  $m$  and  $n$  control the wavelet dilation and translation, respectively;  $a_0$  is the dilation step parameter and  $b_0$  is the location parameter.

Another function is named as the scaling function and is related with the smoothing of the signal. The scaling function can be written as

$$\phi_{m,n}(t) = 2^{-m/2} \phi(2^{-m}t - n) \quad (3.6)$$

$\phi_{0,0} = \phi(t)$  is termed as the father wavelet. Approximation coefficients are found using the scaling function as follows



$$S_{m,n} = \int_{-\infty}^{\infty} x(t) \phi_{m,n}(t) dt \quad (3.7)$$

A signal can be represented by using both approximation coefficients and wavelet coefficients (detail coefficients) via the following expression

$$x(t) = \sum_{n=-\infty}^{\infty} S_{m_0,n} \phi_{m_0,n}(t) + \sum_{m=-\infty}^{m_0} \sum_{n=-\infty}^{\infty} T_{m,n} \psi_{m,n}(t) \quad (3.8)$$

We can see from this equation that the original continuous-time signal  $x(t)$  is expressed as a linear combination of its approximation at an arbitrary scale index  $m_0$  and a an infinite number of detail terms from  $-\infty$  to scale  $m_0$ . An image is a two-dimensional signal. Therefore, the two-dimensional scaling function can be written as

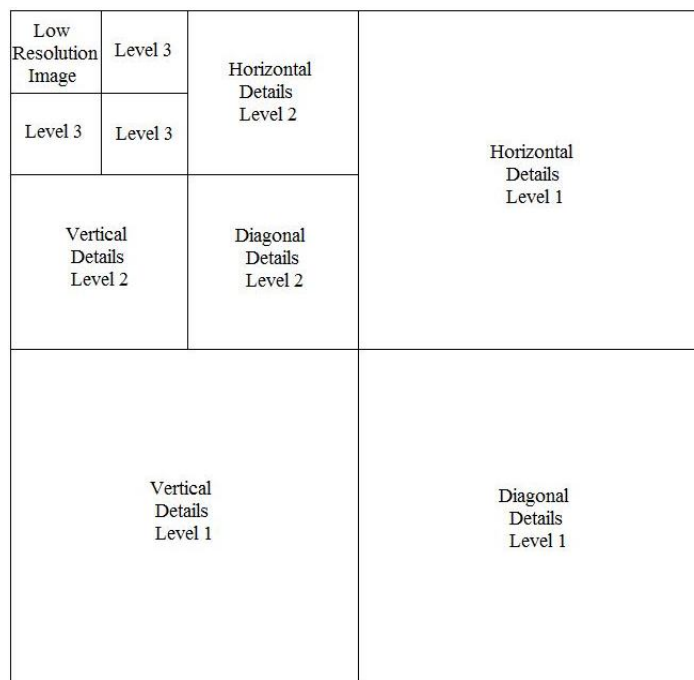
$$\phi(t_1, t_2) = \phi(t_1)\phi(t_2) \quad (3.9)$$

Accordingly, the two-dimensional horizontal, vertical, and diagonal wavelets are expressed as

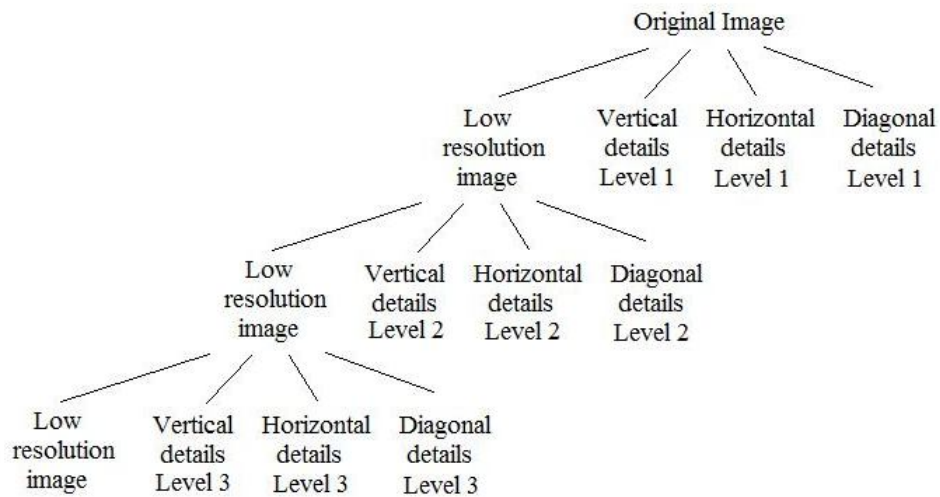
$$\begin{aligned} \psi^h(t_1, t_2) &= \phi(t_1)\psi(t_2) \\ \psi^v(t_1, t_2) &= \psi(t_1)\phi(t_2) \\ \psi^d(t_1, t_2) &= \psi(t_1)\psi(t_2) \end{aligned} \quad (3.10)$$

DWT is obtained by applying a series of low pass and high pass filtering to the original signal. Then, these filter outputs are downsampled. High pass filtering gives the detail components of the image. In order to obtain the detail components, image is high pass filtered at horizontal, vertical, and diagonal directions and the detail components are obtained at these directions. Low pass filtering of the image gives the approximation components (low resolution image).

In this thesis, a 3-level DWT is applied. 3-level wavelet decomposition of an image is illustrated in Figure 3.3 below.



a)



b)

Figure 3.3 (a) and (b) 3-level wavelet decomposition.

### 3.3 Region Based Features

Image Processing Toolbox of Matlab is used to extract features from image regions. First, we have to define what we mean by “region”. In Figure 3.4 below, a region corresponds to the white pixels and the yellow box represents the bounding box.

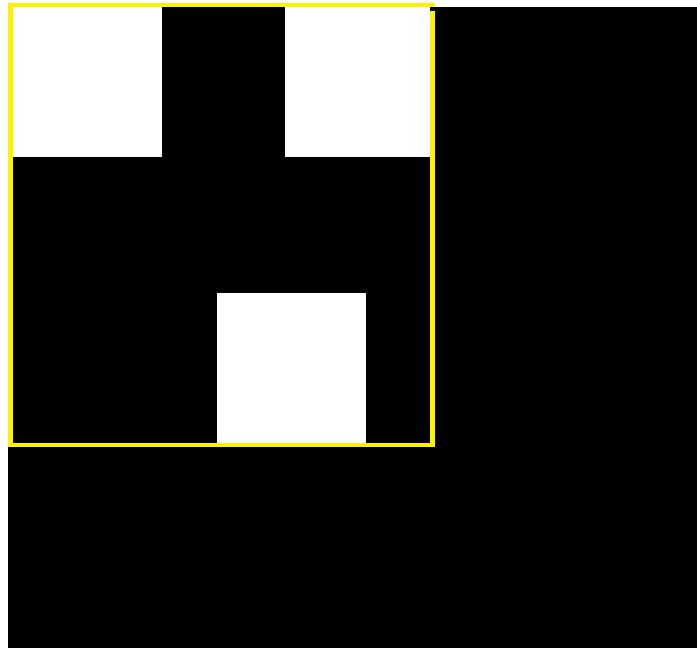


Figure 3.4 Region and bounding box.

12 region based features are extracted from images. These features are area, major axis length, minor axis length, eccentricity, orientation, convex area, filled area, Euler number, equiv diameter, solidity, extent, and perimeter. Short descriptions of these region based features are given below as defined in (MATLAB Image Processing Toolbox, R2011a Documentation, 2011).

*Area:* This feature gives the actual number of pixels in the region.

*Major Axis Length:* Specifying the length (in pixels) of the major axis of the ellipse that has the same normalized second central moments as the region.

*Minor Axis Length:* Specifying the length (in pixels) of the minor axis of the ellipse that has the same normalized second central moments as the region.

*Eccentricity:* Specifying the eccentricity of the ellipse that has the same second moments as the region. The eccentricity is the ratio of the distance between foci of the ellipse and its major length. This can be represented as

$$e = \sqrt{\frac{a^2 - b^2}{a^2}} = \sqrt{1 - \left(\frac{b}{a}\right)^2} \quad (3.11)$$

The distance between the center and one of two foci is equal to  $\sqrt{a^2 - b^2}$  with  $a$  and  $b$  as shown in Figure 3.5.

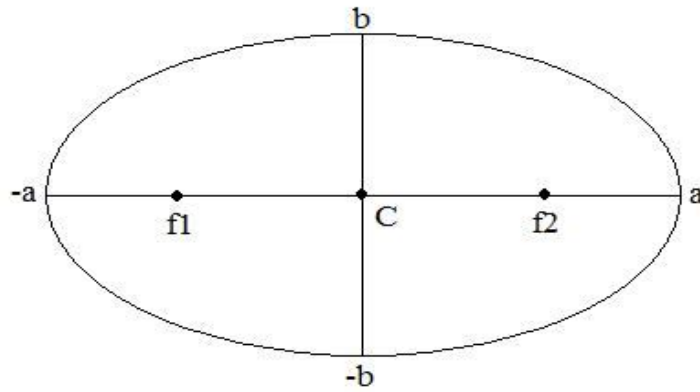


Figure 3.5 Ellipse.

*Orientation:* Specifying the angle from -90 to 90 degrees between the x-axis and the major axis of the ellipse that has the same second moments as the region.

*Convex Area:* Specifying the number of pixels in convex image. Convex image is the binary image that specifies the convex hull, with all pixels within the hull filled in. Convex hull is the smallest convex polygon that can contain the region.

*Filled Area:* Specifying the number of “on” pixels in filled image. The “on” pixels in filled image correspond to the region, with all holes filled in.

*Euler Number:* Specifying the number of objects in the region minus the number of holes in those objects.

*EquivDiameter*: Specifying the diameter of a circle with the same area as the region.

*Solidity*: Specifying the proportion of the pixels in the convex hull that are also in the region. It is computed as Area/Convex Area.

*Extent*: Specifying the ratio of pixels in the region to pixels in the total bounding box. It is obtained by dividing the Area to the area of the bounding box.

*Perimeter*: The distance around the boundary of the region.

### 3.4 Nondestructive Laboratory Testing

6 features were obtained by nondestructive laboratory testing methods in the research project TÜBİTAK MAG 104M358. These 6 features are max pulse wave velocities ( $m/s$ ), anisotropy, area ratios overall, unit weights ( $gr/cm^3$ ), effective porosity (%), eccentricity as vector ( $cm$ ) which are determined for all the marble samples in the dataset. In fact, two of these six features (area ratios overall and eccentricity) are obtained by image processing techniques. Nonetheless, in this thesis, these two features are mentioned inside nondestructive laboratory testing methods to be consistent with the categorization in (Selver, et al., 2008). The values and descriptions of these features are borrowed from the work (Selver, et al., 2008).

*Max Pulse Wave Velocity*: Max pulse wave velocity is measured by applying ultrasonic waves to opposite faces of each marble cube in three orthogonal directions. Pulse wave velocity is determined as

$$MaxPWV = \frac{CubeThickness}{PulseTransitionTime} \quad (3.12)$$

*Anisotropy*: The anisotropy parameter was defined as a feature in order to capture the anisotropic nature of the specimen by taking the difference between the highest and lowest pulse wave velocities measured along any three orthogonal directions.

*Overall Area Ratio:* This feature is determined using image processing techniques. Images of the six faces of each cubic sample are first captured and the area of breccia grains is calculated with Otsu thresholding method (Otsu, 1979). We should mention that the most satisfactory visual results of images of cubic marble samples with Otsu thresholding method are obtained for samples in Group 3. Therefore, the threshold value obtained for Group 3 is applied to all groups of cubic marble samples. Ratio of this area to the total surface area of the cubic specimen is defined as the Overall Area Ratio feature. It should be noted that this parameter is unity for fully homogeneous limestone specimens. It is important to note that UCS decreases as the numeric value of this feature decreases.

*Unit Weights:* Unit weights are also measured experimentally since the cubic samples are not exact cubes and geometric calculation of the volume would be misleading. Volume information of each sample is determined using the Archimedes principle. Volume is the difference between the dry weight ( $W_{dry}$ ) and the weight of the water ( $W_{water}$ ), which is overflowed by the sample under the assumption that density of water is  $1 \text{ g / cm}^3$ .

$$UnitWeight = \frac{W_{dry}}{W_{dry} - W_{water}} \quad (3.13)$$

*Effective Porosity:* Effective porosity feature is defined as the ratio of the volume of voids inside a sample to the total volume of the sample. Volume of voids is determined using the results of water absorption experiment as

$$V_{voids} = \left( \frac{W_{saturated} - W_{dry}}{\gamma_{water}} \right) \quad (3.14)$$

where  $\gamma_{water}$  is the density of water. In general, UCS decreases as the effective porosity increases.

*Eccentricity:* The eccentricity feature is a planar parameter defined as the deviation of the centroid of all breccia grains on one surface of the cube from the center. This feature is computed for each surface of a sample.

### 3.5 Feature Selection

Dimension of data can be reduced by using feature selection methods. Feature selection is defined as selecting a subset of the existing features without a transformation (Gutierrez-Osuna, 2008a). It is also called feature subset selection. In large datasets, it is needed to reduce the dimension in order to decrease evaluation time. Another advantage of using feature subset selection is increasing the performance of classifier or system because the most meaningful features are selected with feature subset selection. Features that optimize the objective function,  $J$ , are selected for the subset

$$\begin{bmatrix} x_1 \\ x_2 \\ \vdots \\ \vdots \\ x_N \end{bmatrix} \xrightarrow[\text{feature selection}]{} \begin{bmatrix} x_{i_1} \\ x_{i_2} \\ \vdots \\ x_{i_M} \end{bmatrix} \quad (3.15)$$

$$\{x_{i_1}, x_{i_2}, \dots, x_{i_M}\} = \arg \max_{M, i_M} [J\{x_i \mid i = 1 \dots N\}] \quad (3.16)$$

In this thesis, the objective function,  $J$ , is defined as the percentage success in the prediction of UCS. Therefore, the feature subset is selected in order to maximize this percentage success. Alternatively, it can also be said that the feature subset is selected in order to minimize the percentage error in the prediction of UCS.

There are various feature subset selection methods which differ from each other based on their search strategies. A search strategy is needed to direct the feature subset selection process as it explores the space of all possible combinations of features. Search strategies can be divided into 3 categories. These are exponential algorithms, sequential algorithms, and randomized algorithms. Exponential algorithms evaluate a number of subsets that grows exponentially with the dimensionality of the search space. Sequential algorithms add or remove features sequentially, but have a tendency to become trapped in local minima. Randomized algorithms incorporate randomness into their search procedure to escape local

minima. Different search strategies are tabulated in Figure 3.6 under these three categories.

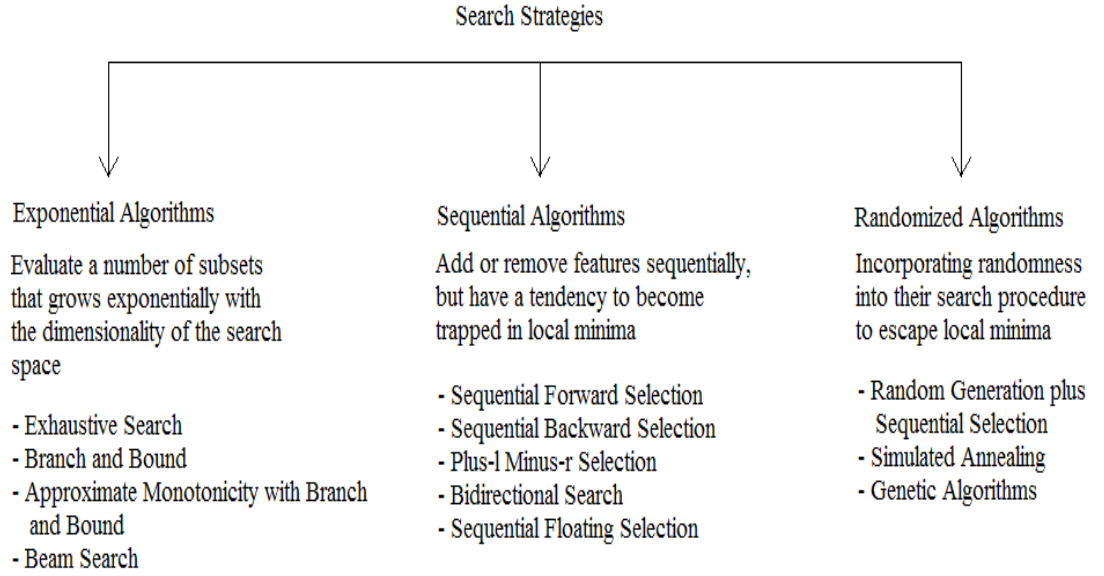


Figure 3.6 Search strategies (Gutierrez-Osuna, 2008a).

One of the sequential search strategies is used in order to decrease the number of marble features and to find the most meaningful ones (when used together). The name of this method is sequential forward selection. Sequential forward selection (SFS) is one of the simplest greedy search algorithms (Gutierrez-Osuna, 2008a). This algorithm starts from an empty set. Then, it adds one feature that optimizes the objective function. It continues adding features to the dataset, sequentially, that maximizes the objective function when used together with features in the data set. Steps of the SFS algorithm are given as:

- 1- Start with the empty set  $Y_0 = \{\emptyset\}$
- 2- Select the next best feature  $x^+ = \arg \max_{x \notin Y_k} [J(Y_k + x)]$
- 3- Update  $Y_{k+1} = Y_k + x^+; k = k + 1;$
- 4- Go to 2.



Above,  $Y_k$  contains the features that have already been selected (Gutierrez-Osuna, 2008a).

As the most important disadvantage of the SFS, it can be stated that it is unable to remove features which are added and decrease the performance after adding new features.

## **CHAPTER FOUR**

### **NEURAL NETWORKS AND LEARNING METHODS**

In this chapter, neural networks and learning methods are studied. A neural network using information obtained from various features determines UCS of a cubic marble sample. As a neural network, multilayered perceptron (MLP), one of the supervised neural networks, is utilized in this thesis. Different learning methods used for training the neural network are bootstrap, K-fold, leave-one-out, and random sub-sampling. These methods are also presented in this chapter.

#### **4.1 Neural Networks**

Neural networks are used in engineering extensively, especially in recent years. They were designed by imitating the human brain. Like human brain, neural networks consist of neurons and can learn what are presented to them as stimuli, and they can interpret new information in light of previous knowledge. As stated in (Haykin, 1999), a neural network is a machine that is designed to model the way in which the human brain performs a particular task or function of interest.

Learning methods of neural networks can be divided into two broad categories. These are described as learning with a teacher and learning without a teacher. Learning with a teacher can also be named as supervised learning and can be thought as learning by means of a teacher. As can be seen in Figure 4.1, the teacher controls learning process of neural network.

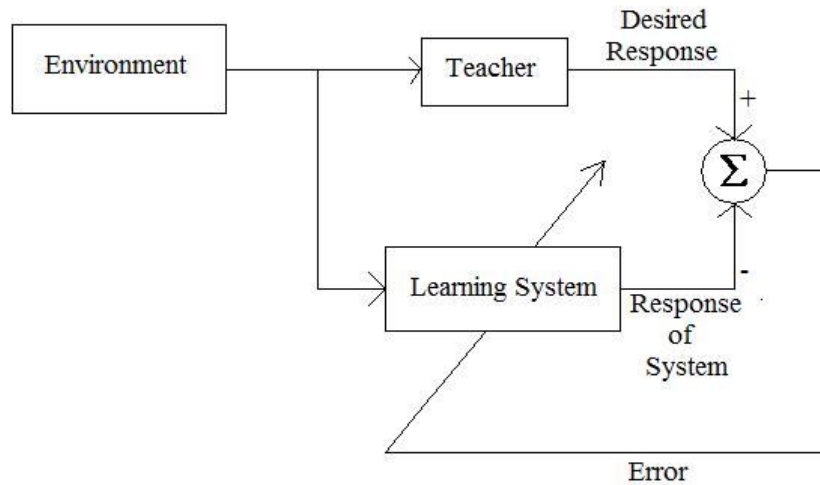


Figure 4.1 Supervised learning.

In conceptual terms, we may think of the teacher as having knowledge of the environment, with that knowledge being represented by a set of input-output examples (Haykin, 1999). Training dataset is used in order to train the neural network. The teacher knows responses of the system to these training data inputs. Neural network is trained according to difference between the desired response provided by the teacher and the response of the system. Therefore, neural networks are trained under the control of the supervisor. As its name implies, learning without a teacher does not use a teacher to control the learning process. There are two types of learning methods in this category. One of them is named as reinforcement learning and the other is named as unsupervised learning.

In this thesis, MLP, a popular member of supervised neural networks, is used.

#### ***4.1.1 Multilayered Perceptrons***

MLP is a widely used neural network type. It has three parts. These are the input layer, the hidden layer, which can be more than one, and the output layer. Input vector is presented to the network via input layers. By means of hidden layers, neural network obtains nonlinear results because the hidden layer can use nonlinear activation functions. As understood from its name, the output layer produces the response of the neural network to the input vector. An MLP structure, with one hidden layer, can be seen in Figure 4.2.

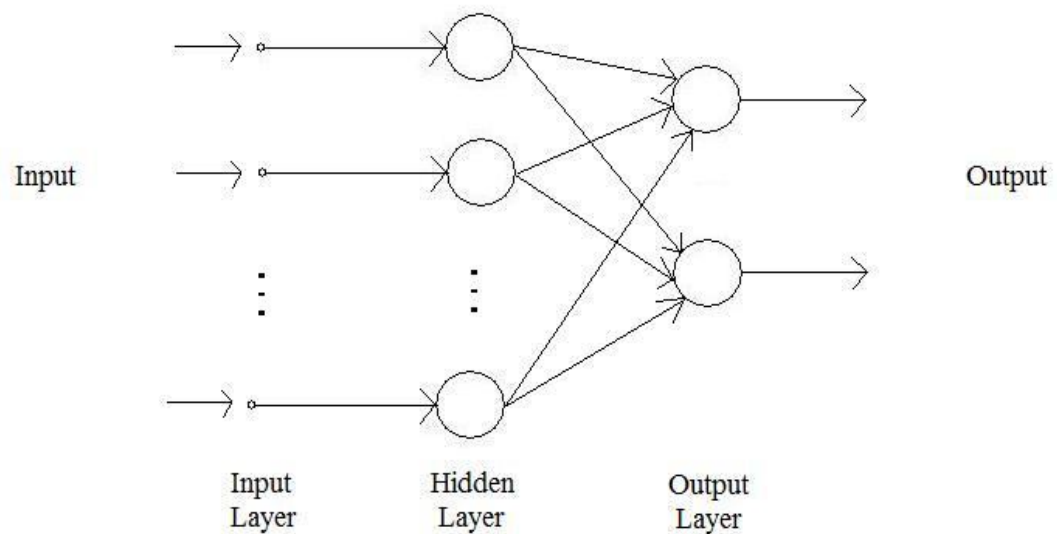


Figure 4.2 Structure of an MLP with one hidden layer.

Each node is named as neuron in neural networks. In Figure 4.2, one neuron is connected to all neurons in the previous layer. This type of network is named as full-connected network. All neurons are connected by synaptic weights. MLP is trained via error back-propagation algorithm. This algorithm is based on an error-correction learning rule (Haykin, 1999). The error back-propagation algorithm has two passes. One of them is forward pass and the other is backward pass. In forward pass, output is evaluated for input data that are supplied from the input layer. Synaptic weights are fixed in forward pass. The difference between the desired response and the output obtained from the forward pass gives the error signal. This error signal is used to adjust the synaptic weights. The error signal is propagated backward through the network. The synaptic weights are set to their new values by this way. The synaptic weights are adjusted in order to obtain the minimum difference between the desired response and the output of the network (Haykin, 1999). If summarized, first of all, input is presented to neural network. Then, output is calculated for this input vector. After the error signal is calculated from the desired output and current response, synaptic weights are adjusted according to error signal until the error signal approaches zero.

There are various types of backpropagation algorithms. In this thesis, as in (Ardali, 2008), the gradient descent backpropagation with adaptive learning rate is used in simulations.

## 4.2 Learning Methods

The process of using the entire training data to select the optimal predictor and then estimating the error rate has a major drawback. The final model will over-fit the training data limiting the generalization capability of the system. Hence, the error rate estimate will be lower than the true error rate. To remedy this situation, several learning methodologies have been proposed in the literature including holdout, random sub-sampling, K-fold cross-validation, leave-one-out cross-validation, and bootstrap (Figures 4.3 and 4.4). These learning methodologies are also studied in (Selver, et al., 2008).

*Holdout:* The Holdout method partitions the data into two subsets called a training set and a test set or holdout set (Figure 4.3(a)). It is common to designate 2/3 of the data as the training set and the remaining 1/3 as the test set. The training set is given to the inducer, and the induced classifier is tested on the test set. The holdout method has two basic drawbacks. Firstly, in problems with a sparse data set, it may not be possible to set a portion of the dataset in which samples for training and testing are homogeneously distributed to represent the characteristics of the dataset. Secondly, it is a single train-and-test experiment that can result in misleading error rate estimation due to “fortunate” or “unfortunate” splits. The limitations of the holdout method can be overcome with a family of re-sampling methods at the expense of higher computational cost.

*Random Sub-Sampling:* Random sub-sampling performs K data splits of the entire dataset (Figure 4.3(b)). Each data split randomly selects a fixed number of examples without replacement. For each data split, classifier is trained and tested. Then, the true error estimate is obtained as the average of the separate estimates.

*K-Fold Cross Validation:* In this methodology, a K-fold partition of the dataset is created (Figure 4.3(c)). For each of K experiments, K-1 folds are used for training

and a different fold for testing. K-fold cross validation is similar to random sub-sampling. The advantage of K-fold cross validation is that all the examples in the dataset are eventually used for both training and testing.

*Leave-One-Out:* Leave-one-out is the degenerate case of K-fold cross validation, where  $K$  is chosen as the total number of examples. For a dataset with  $N$  examples,  $N$  experiments are performed. For each experiment,  $N-1$  examples are used for training and the remaining example is used for testing (Figure 4.3(d)). Then, the true error estimate is obtained as the average of the separate estimates again.

*Bootstrap:* The bootstrap is a re-sampling technique with replacement (Figure 4.4). From a dataset with  $N$  examples, all examples are randomly selected with replacement. This set of examples is used for training and the remaining examples that were not selected for training are used for testing. This process is repeated for a specified number of folds ( $K$ ). As before, the true error is estimated as the average error rate on test examples. It is worthwhile to point out that a different number of samples might probably be used for training and testing at each experiment.

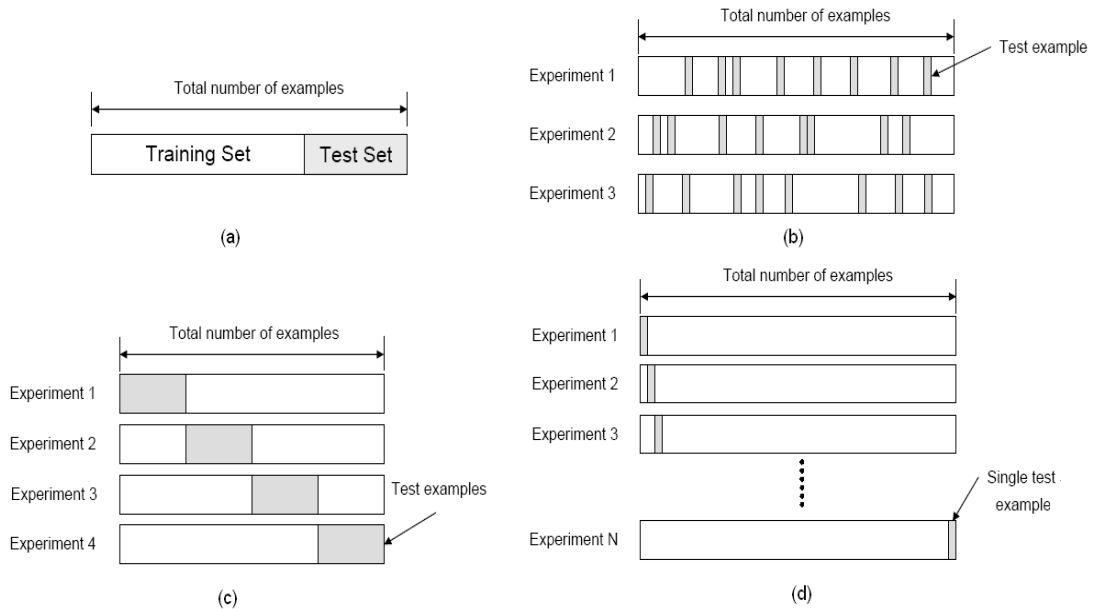


Figure 4.3 Learning schemes for (a) holdout (b) random sub-sampling (c) K-fold (d) leave-one-out cross validation methods (Gutierrez-Osuna, 2008b).



Figure 4.4 Learning scheme for the bootstrap method (Gutierrez-Osuna, 2008b).

## **CHAPTER FIVE**

### **SIMULATION RESULTS**

Results of the performed simulations are summarized in this chapter. Simulations are accomplished by using MATLAB and its various toolboxes. Results obtained by using different features are given in different sections. These results are also compared with previous results of similar works in the literature.

There are a limited number of works in the literature to determine the qualitative and quantitative properties of natural stones. In (Ardali, 2008), the marble dataset was used to separate the marbles into their quality groups by using textural SDH and spectral wavelet features. In this thesis, UCS values of cubic marble samples are determined using the same marble dataset. In (Selver, et al., 2008), axial strength is tried to be estimated by using various features obtained by nondestructive laboratory tests. In this thesis, in addition to these features, SDH, wavelet, and region based features of marble surface images are also used. All these additional features are formed by various image processing techniques.

In this thesis, MLP is used as the neural network type in simulations. MLP parameters are different for each feature extraction method. For example, the epoch number is 500 for SDH features. This value is found after trying out different epoch numbers (for instance, 200, 500, 1000, 1500, 2000). Then, one of them giving better results is determined and used as the suitable epoch number for the SDH method. This process is performed for each feature extraction method.

In simulations, feature selection is performed to reduce the dimension and increase the performance of MLP. For this aim, sequential forward selection is used. Results of simulations with feature selection and without feature selection are compared. In order to accomplish sequential forward selection on marble data, Monte Carlo simulation methods are used because one realization is not sufficient to get trustworthy inference from the results. There are various reasons for that. One reason is regarding selection of train and test data for the neural network. It is



obvious that the simulation results can be different for each run because of different train and test data sets. For each realization, train and test data are selected and then the neural network is trained. This process is repeated 30 times. Thus, neural network is trained with 30 different train and test datasets. On the other hand, the number of realizations for wavelet features is different from other features because 30 runs are not enough to provide satisfactory results for wavelet features. In order to apply the feature selection algorithm to wavelet features, the number of realizations is increased to 90 to get more stable and meaningful results.

Results are obtained for different learning methods briefly introduced in the previous chapter. In the simulations, number of experiments for bootstrap and random sub-sampling method is selected as 10 and K-fold method is performed as 10-fold.

### 5.1 Determination of UCS Using Sum and Difference Histogram (SDH) Features

SDH method is used to extract textural features in order to use for determining the axial strength of cubic marble samples. Extraction of SDH features was explained in Chapter 3. The dataset consists of colored images. Therefore, the color space has 3 channels. In this work, the color space is selected as RGB which has integer gray level values in the range [0, 255]. Accordingly, all pixel values are between 0 and 255.

SDH are found for red, green, and blue color channels. Sum and difference histogram vectors have the size of  $1 \times 511$  because there are 256 gray levels. Therefore, the size of the vectors becomes  $(2 \times N_g) - 1 = 511$ . 7 statistical features are calculated from SDH for these 3 color channels. Therefore, there are 21 ( $7 \times 3 = 21$ ) features for one surface image. A marble cube has 6 surfaces. Thus, there are 126 features ( $21 \times 6 = 126$ ) in total for one marble cube to determine its UCS. Before their use, normalization is also applied to the features. Normalization is accomplished via the following expression

$$x_{new} = \frac{x - \mu}{\sigma} \quad (5.1)$$

where  $x_{new}$  is the new value of a feature after normalization and  $\mu$  and  $\sigma$  are the mean value and standard deviation, respectively, of that feature. This normalization is applied for all features of 157 marble cubes.

MLP is used to predict axial strength with 500 epochs and 5 neurons in the hidden layer. If all 126 SDH features are used to determine the axial strength of a marble cube, performance results (in terms of percentage error) for training and test phases are obtained as in Table 5.1.

Table 5.1 Performance results (percentage error) of training and test using all 126 SDH features.

Training				
157 Samples 126 Features				
	Bootstrap	10 Fold	Leave One-out	Random sub.
<b>Min</b>	7.8326	9.7750	9.7291	9.8771
<b>Max</b>	10.7105	11.8514	12.9315	11.9773
<b>Mean</b>	9.2232	10.8586	11.3301	10.9499
<b>Std</b>	0.9116	0.6531	0.6140	0.6603

Test				
157 Samples 126 Features				
	Bootstrap	10 Fold	Leave One-out	Random sub.
<b>Min</b>	15.2685	11.9823	0.1527	12.1731
<b>Max</b>	21.4787	24.6880	78.4283	23.4918
<b>Mean</b>	18.0697	17.9899	16.9185	17.2089
<b>Std</b>	1.9307	3.9693	14.9479	3.6104

Then, feature selection method is applied to 126 SDH features. After 30 sequential forward selection realizations, some features are not selected within these 30 realizations. Therefore these features (107 features in total) are eliminated. The remaining 19 features are selected at least in 1 realization out of 30. In this work, features that are selected in more than 3 realizations out of 30 (10% of Monte Carlo realizations) are decided to be determined as the final remaining features. As a result,

the number of selected features decreased further to 9 from 19. If the neural network is fed only with these remaining 9 features, performance results become as in Table 5.2.

After applying feature selection, a small decrease occurred in percentage error for test data while a small increase occurred for training data. Although error increased for training data, the important parameter is test performance. Error is decreased between 1 and 2 % for different learning methods in the test phase.

Table 5.2 Performance results of training and test for 9 SDH features obtained after feature selection.

Training				
157 Samples 9 Features				
	Bootstrap	10 Fold	Leave One-out	Random sub.
<b>Min</b>	11.9557	12.8360	12.8814	13.0017
<b>Max</b>	14.6625	14.6513	15.6853	14.8210
<b>Mean</b>	13.2712	13.6992	13.8948	13.8290
<b>Std</b>	0.8593	0.5711	0.4885	0.5593

Test				
157 Samples 9 Features				
	Bootstrap	10 Fold	Leave One-out	Random sub.
<b>Min</b>	13.5113	10.4448	0.1317	11.3529
<b>Max</b>	18.5161	23.6987	71.2366	21.0231
<b>Mean</b>	15.9606	16.9875	15.4126	15.9371
<b>Std</b>	1.5435	4.4207	12.8949	3.1294

## 5.2 Determination of UCS Using Wavelet Features

Wavelet features are also used to determine the axial strength of marble samples. Wavelet analysis is performed on gray level marble surface images. 3-level discrete wavelet decompositions are performed. Features are extracted by using approximation and detail coefficients (vertical, horizontal, and diagonal detail

coefficients) at each decomposition level after applying DWT. These features are mean, median, and variance, as in (Ardalı, 2008). Thus, mean, median, and variances of wavelet analysis coefficients are used as wavelet features. By this way, 30 features are obtained for one marble surface image. Since a marble cube has 6 faces, the number of features to determine the axial strength of a cubic marble sample is 180 ( $6 \times 30 = 180$ ). Then, normalization is applied to these features as explained in the previous section.

MLP is used to predict UCS with 500 epochs and 10 neurons in the hidden layer. Simulations are performed for different learning methods. If all 180 wavelet features are used to determine the axial strength of a marble cube, percentage error performance results of training and test phases are obtained as in Table 5.3 below.

Table 5.3 Performance results of training and test phases for all 180 wavelet features.

Trainig				
157 Samples 180 Features				
	Bootstrap	10 Fold	Leave One-out	Random sub.
<b>Min</b>	4.0961	6.3364	6.4767	6.5780
<b>Max</b>	6.8499	9.1371	11.2978	9.0798
<b>Mean</b>	5.2500	7.6918	8.3905	7.7703
<b>Std</b>	0.8898	0.8872	0.8236	0.7979

Test				
157 Samples 180 Features				
	Bootstrap	10 Fold	Leave One-out	Random sub.
<b>Min</b>	21.5585	13.9866	0.2829	14.3592
<b>Max</b>	40.7524	64.5905	193.9286	38.9229
<b>Mean</b>	29.4934	29.0348	22.7014	23.7734
<b>Std</b>	6.2439	16.3567	24.9491	7.5822

Feature selection method is also applied to 180 wavelet features. After 90 sequential forward selection realizations, some features are not selected within these 90 realizations. Therefore these features (124 features) are eliminated. The remaining

56 features are selected at least in 1 realization out of 30. In this work, features that are selected in more than 9 realizations out of 90 (10% of Monte Carlo realizations) are determined as final remaining features. Thus, the number of selected features decreased further to 3 from 180. When the neural network is simulated using only these 3 remaining features, the obtained performance results are given in Table 5.4.

Table 5.4 Performance results of training and test phases for 3 wavelet features obtained after feature selection.

Trainig				
157 Samples 3 Features				
	Bootstrap	10 Fold	Leave One-out	Random sub.
<b>Min</b>	12.3368	13.1234	12.8743	13.2539
<b>Max</b>	15.5304	15.7020	17.4848	15.7719
<b>Mean</b>	13.8353	14.2343	14.4088	14.2985
<b>Std</b>	0.9999	0.7779	0.7820	0.8042

Test				
157 Samples 3 Features				
	Bootstrap	10 Fold	Leave One-out	Random sub.
<b>Min</b>	13.3841	11.4113	0.1320	10.8354
<b>Max</b>	19.4641	23.8459	68.7618	21.0714
<b>Mean</b>	16.0869	17.1722	15.5516	15.5534
<b>Std</b>	1.9305	3.9833	12.7428	3.1716

As seen from Tables 5.3 and 5.4, after applying feature selection, a significant decrease occurred in percentage error for the test phase while in the training phase percentage error increased. Hence, we can state that feature selection gives satisfactory results for features obtained from wavelet analysis because test phase matters the most. Error is decreased between 7 and 13% for different learning methods for the test phase.

Before applying feature selection, simulations for 180 wavelet features give worse results than using 126 features of SDH. However, after applying feature selection, performance results of wavelet analysis and SDH get close to each other.

### 5.3 Determination of UCS Using Region Based Features

Regional properties of marble surface images are also used to extract features for determining UCS. These region based features are obtained to exploit the suspected relationship between some regional properties such as location, area, shape, etc. and the axial strength. In order to accomplish that, 12 features are extracted. These 12 features belong to one marble surface image. Considering all 6 faces of a marble cube, the total number of region based features for one cubic marble sample is found as 72 ( $6 \times 12 = 72$ ).

MLP is used to predict UCS with 2500 epochs and 10 neurons in the hidden layer. If all 72 features are used, error percentage performance results of training and test phases can be seen in Table 5.5.

Table 5.5 Performance results of training and test phases for all 72 region based features.

Training				
157 Samples 72 Features				
	Bootstrap	10 Fold	Leave One-out	Random sub.
<b>Min</b>	8.0958	9.6789	9.8795	9.9478
<b>Max</b>	10.8428	11.8703	12.7083	11.8506
<b>Mean</b>	9.5059	10.7759	11.1649	10.8620
<b>Std</b>	0.8689	0.6991	0.5514	0.6065

Test				
157 Samples 72 Features				
	Bootstrap	10 Fold	Leave One-out	Random sub.
<b>Min</b>	15.4947	12.0091	0.1544	11.6608
<b>Max</b>	23.9669	29.4330	101.8957	23.9998
<b>Mean</b>	19.0570	18.5446	17.0176	17.1567
<b>Std</b>	2.6301	5.3592	16.5742	4.0005

Again, feature selection is applied to 72 region based features. After 30 sequential forward selection realizations, some features are not selected within these 30 realizations. Therefore these features (56 features) are eliminated. The remaining 16 features are selected in at least 1 realization out of 30. In this thesis, features that are selected in more than 3 realizations out of 30 (10% of Monte Carlo realizations) are determined as the final remaining features. As a result, the number of selected features decreased further to 7 from 16. If the neural network is simulated with these 7 remaining features, performance results are obtained as in Table 5.6.

Table 5.6 Performance results of training and test phases for 7 remaining region based features after feature selection.

Training				
157 Samples 7 Features				
	Bootstrap	10 Fold	Leave One-out	Random sub.
<b>Min</b>	11.3371	12.3356	12.0919	12.3558
<b>Max</b>	13.7746	14.1345	14.4492	14.1424
<b>Mean</b>	12.5445	13.2107	13.4290	13.2642
<b>Std</b>	0.7622	0.5690	0.4782	0.5633

Test				
157 Samples 7 Features				
	Bootstrap	10 Fold	Leave One-out	Random sub.
<b>Min</b>	13.7828	11.6819	0.1700	11.4080
<b>Max</b>	18.9914	23.9435	87.9040	21.2564
<b>Mean</b>	16.4158	17.2603	15.6082	15.9982
<b>Std</b>	1.6947	4.2322	13.9772	3.1932

As can be seen from Tables 5.5 and 5.6, after applying feature selection, a small decrease occurs in percentage error for the test phase while a small increase is seen for the training phase. This behavior is analogous to SDH features. Error is decreased between 1 and 2.5 % for different learning methods for the test phase.

After applying feature selection, it can be noticed that the performance results of region based features and wavelet features become very close to each other.

#### 5.4 Determination of UCS Using Nondestructive Laboratory Testing

Features via nondestructive laboratory testing methods were extracted previously in (Selver, et al., 2008). In this thesis, although the total number of these features is not large, feature selection is still performed to further reduce the number of features. The obtained performance results are compared with that of (Selver, et al., 2008). Features that are obtained via nondestructive laboratory tests were introduced in Chapter 3. These 6 features are max pulse wave velocities ( $m/s$ ), anisotropy, area ratios overall, unit weights ( $gr/cm^3$ ), effective porosity (%), eccentricity as vector ( $cm$ ), each belonging to one cubic marble sample. Normalization is also applied to these features.

MLP is used to predict UCS with 2500 epochs and 10 neurons in the hidden layer. If all 6 features are used, error percentage performance results of training and test phases can be seen in Table 5.7.



Table 5.7 Performance results of training and test phases for all 6 features of nondestructive laboratory tests.

Training				
157 Samples 6 Features				
	Bootstrap	10 Fold	Leave One-out	Random sub.
<b>Min</b>	10.2569	11.3663	11.3034	11.4362
<b>Max</b>	12.7831	13.1703	14.0321	13.0961
<b>Mean</b>	11.4700	12.1918	12.3803	12.2237
<b>Std</b>	0.7831	0.5760	0.4886	0.5313

Test				
157 Samples 6 Features				
	Bootstrap	10 Fold	Leave One-out	Random sub.
<b>Min</b>	13.0616	10.3884	0.1197	10.0162
<b>Max</b>	19.0595	20.8925	95.6797	21.3607
<b>Mean</b>	16.0740	15.0046	15.1737	15.0680
<b>Std</b>	1.9368	3.3535	14.5161	3.5743

Feature selection is also applied to 6 nondestructive laboratory test features. After 30 sequential forward selection realizations, some features are not selected within these 30 realizations. Therefore these features are eliminated. In this work, features that are selected in more than 3 realizations out of 30 (10% of Monte Carlo realizations) are determined as the final remaining features. As a result, the number of selected features decreased further to 3 from 6. When the neural network is simulated with these 3 remaining features, error percentage performance results are obtained as in Table 5.8.

Table 5.8 Performance results of training and test phases for 3 remaining features of nondestructive laboratory tests.

Training				
157 Samples 3 Features				
	Bootstrap	10 Fold	Leave One-out	Random sub.
<b>Min</b>	11.1165	12.0859	11.9514	12.0282
<b>Max</b>	13.4644	13.5001	14.6910	13.4631
<b>Mean</b>	12.2990	12.7334	12.8480	12.7367
<b>Std</b>	0.7198	0.4543	0.4172	0.4495

Test				
157 Samples 3 Features				
	Bootstrap	10 Fold	Leave One-out	Random sub.
<b>Min</b>	12.3250	9.8986	0.1624	10.2310
<b>Max</b>	17.9020	18.9832	60.8726	19.0812
<b>Mean</b>	14.8451	14.0695	14.2403	14.3626
<b>Std</b>	1.6885	2.8518	12.0776	2.8438

As seen from Tables 5.7 and 5.8, after applying feature selection, a small decrease occurred in percentage error for the testing phase while a small increase occurred for the training phase. Error is decreased approximately 1% for different learning methods during testing.

## CHAPTER SIX

### CONCLUSIONS

In this thesis, signal and image processing techniques are applied to determine UCS of cubic marble samples. For this aim, SDH, wavelet analysis, region based image analysis, and nondestructive laboratory testing methods are used to extract features. These features are presented to MLP network to determine the UCS of marbles. By this way, we were able to eliminate the necessity of using destructive laboratory tests for the same purpose. Finally, rather irrelevant features are eliminated via a feature selection algorithm, thus reducing the dimension considerably.

In (Selver, et al., 2008), prediction of UCS of marbles was performed by using non-destructive laboratory testing methods. In this thesis, as an extension to the nondestructive laboratory test features in that work, new features are extracted by using signal and image processing techniques. Results in (Selver, et al., 2008) and the new results obtained in this thesis support each other, especially after application of feature selection.

In Section 5.1, SDH features are used to determine UCS of marble samples. These features are extracted using RGB color space as in (Ardalı, 2008). Percentage error performance results improve after using only the 9 selected features compared to using all 126 SDH features. Mean, variance, energy, correlation, entropy, contrast, and homogeneity constitute 126 SDH features. However, only mean, energy, and homogeneity appear in 9 selected features.

It could also be of interest to determine which faces of cubic samples the selected features belong to. We also give that information below. For the labeling of faces of cubic samples, we refer to Figure 2.4. After feature selection, the remaining SDH mean features are obtained from the green color channel of 4<sup>th</sup> face, the green color channel of 6<sup>th</sup> face, and the blue color channel of 4<sup>th</sup> face. The remaining SDH energy features are obtained from the red color channel of 2<sup>nd</sup> face, the green color channel

of 2<sup>nd</sup> face, blue color channel of 1<sup>st</sup> face, and the blue color channel of 2<sup>nd</sup> face. The remaining SDH homogeneity features are obtained from the green color channel of 5<sup>th</sup> face and the blue color channel of 2<sup>nd</sup> face.

In Section 5.2, 3-level DWT is applied to obtain wavelet analysis features to determine UCS cubic marble samples. Again, percentage error performance results improve after using only the 3 selected features compared to using all 180 wavelet features. Mean, median, and variance of detail and approximation wavelet coefficients are used in all 180 wavelet features. However, only the median and variance are used in 3 selected features.

After feature selection, wavelet median features are obtained from 2<sup>nd</sup> face 3<sup>rd</sup> level approximation coefficients. Wavelet variance features are obtained from 3<sup>rd</sup> face 3<sup>rd</sup> level approximation coefficients and 5<sup>th</sup> face 3<sup>rd</sup> level approximation coefficients.

The important characteristics of these features are that all of selected wavelet features are obtained from approximation coefficients. That is, if high frequency components of an image are used as feature, the success of determination of UCS decreases. Thus, it can be concluded that use of high frequency components as features is unnecessary. We also would like to note that, for marble surface images, the high frequency components correspond mostly to edges such as thin veins.

In Section 5.3, results of applying region based features are presented for determination of UCS. Similar to SDH and wavelet features, percentage error performance results improve after using only the 7 selected features compared to using all 72 region based features. Area, major axis length, minor axis length, eccentricity, orientation, convex area, filled area, Euler number, equivdiameter, solidity, extent, and perimeter were used in all 72 region based features. However, only area, filled area, and perimeter are used within 7 selected region based features.

After feature selection, region based area features are obtained from 2<sup>nd</sup> and 4<sup>th</sup> faces. Region based filled area features are obtained from 4<sup>th</sup>, 5<sup>th</sup>, and 6<sup>th</sup> faces. Finally, region based perimeter features are obtained from 1<sup>st</sup> and 5<sup>th</sup> faces.

Finally, in Section 5.4, features obtained using nondestructive laboratory tests are applied to determine UCS. As the other feature types, percentage error performance results improve after using only the 3 selected features compared to using all 6 nondestructive laboratory test features. Max pulse wave velocities ( $m/s$ ), anisotropy, area ratios overall, unit weights ( $gr/cm^3$ ), effective porosity (%), and eccentricity as vector ( $cm$ ) were the original 6 nondestructive laboratory test features. However, only max pulse wave velocities ( $m/s$ ), area ratios overall, and effective porosity (%) remained as 3 more relevant and hence selected features.

In Figure 6.1 below, values of 3 selected features versus the cubic marble sample number can be seen. In Figure 6.1(a) UCS values, in Figure 6.1(b) max pulse wave velocities ( $m/s$ ), in Figure 6.1(c) area ratios overall, and in Figure 6.1(d) effective porosity (%) versus the cubic marble sample number can be seen. A correlation between UCS and the 3 selected features obtained after feature selection method is apparent. Therefore, it does not come as a surprise that use of these 3 selected features increases the performance of UCS prediction.

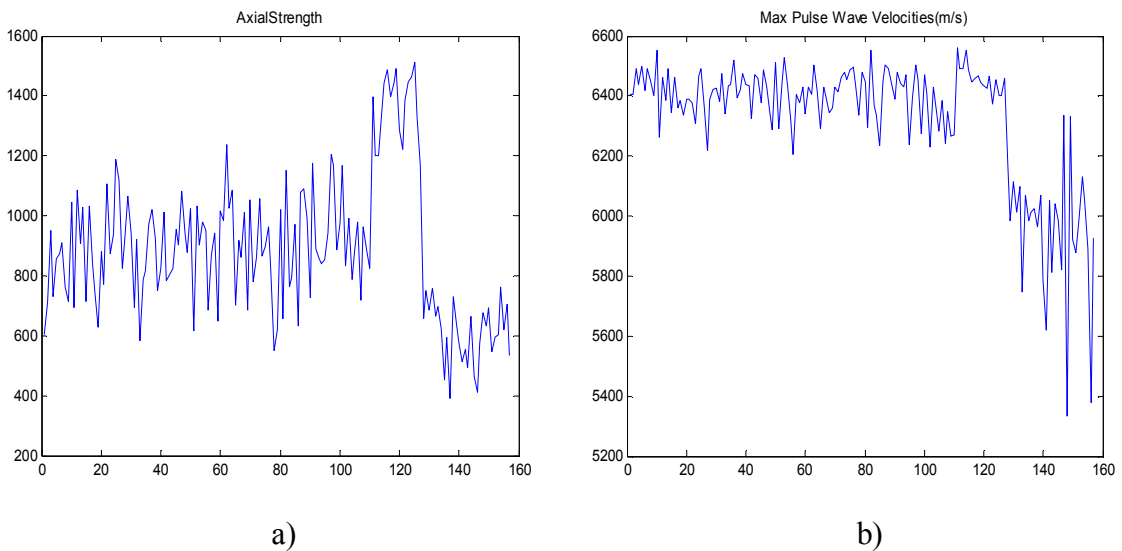


Figure 6.1 (a) Axial strength versus sample number, (b) max pulse wave velocity ( $m/s$ ) versus sample number, (c) area ratios overall versus sample number, and (d) effective porosity (%) versus sample number.

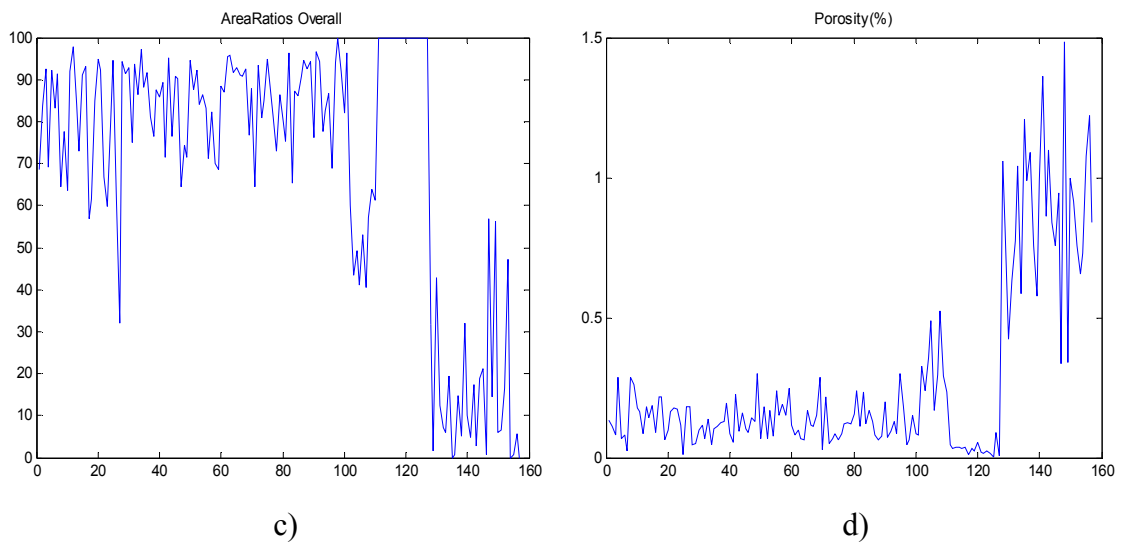


Figure 6.1 (continued)

After feature selection is applied, the numbers of selected SDH, wavelet, and region based features are 9, 3, and 7, respectively. They can also be seen in Table 6.1.

Table 6.1 Numbers of total extracted and selected features.

Features	Number	
	Extracted Features	Obtained After Feature Selection
SDH	126	9
Wavelet Analysis	180	3
Image Region	72	7
NDT	6	3

After feature selection is applied, it is seen that some faces of cubes are used more than others in extraction of selected features. 19 selected features are obtained from SDH, wavelet, and region based features after feature selection. 2 features belong to 1<sup>st</sup> face, 6 features belong to 2<sup>nd</sup> face, 1 feature belongs to 3<sup>rd</sup> face, 4 features belong to 4<sup>th</sup> face, 4 features belong to 5<sup>th</sup> face, and 2 features belong to 6<sup>th</sup> face. A cube has 3 directions, and as can be seen from Figure 2.4, these directions pass through the opposite faces which are 1<sup>st</sup> and 3<sup>rd</sup> faces, 2<sup>nd</sup> and 4<sup>th</sup> faces, and 5<sup>th</sup> and 6<sup>th</sup> faces.

Therefore, 3 features belong to the direction of 1<sup>st</sup> and 3<sup>rd</sup> faces, 10 features belong to the direction of 2<sup>nd</sup> and 4<sup>th</sup> faces, and 6 features belong to the direction of 5<sup>th</sup> and 6<sup>th</sup> faces. It is seen that the highest number of features are obtained from the direction of 2<sup>nd</sup> and 4<sup>th</sup> faces, and the least number of features are obtained from the direction of 1<sup>st</sup> and 3<sup>rd</sup> faces.

In (Önal, 2008) and (Selver, et al., 2008), pulse wave velocity values are measured for 3 directions of cubes. The first direction passes through the 1<sup>st</sup> and 3<sup>rd</sup> faces, the second direction passes through the 2<sup>nd</sup> and 4<sup>th</sup> faces, and the third direction passes through the 5<sup>th</sup> and 6<sup>th</sup> faces. Destructive laboratory test to determine UCS (Figure 1.1) are applied to the marble cubes in the direction that gives the maximum pulse wave velocity value. Therefore, the direction, which has the minimum pulse wave velocity value of a marble cube, and the two faces in this direction are located facing outside in the test machine. There are 157 marble samples in total. Table 6.2 shows the numbers of marble cubes with respect to direction for which the pulse wave velocity is minimum.

Table 6.2 Numbers of marble cubes per direction with minimum pulse wave velocity.

Minimum Pulse Wave Velocity (m/s)	
Direction	Number of Marble Cubes
1 <sup>st</sup> Face – 3 <sup>rd</sup> Face	46
2 <sup>nd</sup> Face – 4 <sup>th</sup> Face	56
5 <sup>th</sup> Face – 6 <sup>th</sup> Face	55

As can be seen from Table 6.2, the greatest number of marbles (56) has the direction of 2<sup>nd</sup> and 4<sup>th</sup> faces with minimum pulse wave velocity. The least number of marble cubes (46) has the direction of 1<sup>st</sup> and 3<sup>rd</sup> faces with the minimum pulse wave velocity. These results are somewhat parallel with the selected SDH, wavelet, and region based features, because 3 selected features belong to 1<sup>st</sup> and 3<sup>rd</sup> faces, 10 features belong to 2<sup>nd</sup> and 4<sup>th</sup> faces, and 6 features belong to 5<sup>th</sup> and 6<sup>th</sup> faces.

In summary, in this thesis, SDH, wavelet, image region based features, and features obtained by nondestructive laboratory tests are used to predict UCS of cubic marble samples replacing destructive laboratory tests. Performances of these methods are determined with and without feature selection. It is seen that after the feature selection method is applied, percentage error performance improves, especially for wavelet analysis features. Moreover, performances of different types of features get close to each other. After feature selection is applied, the best performance for UCS prediction is obtained by using the selected nondestructive laboratory test features.

Different types of learning methods are also investigated. After feature selection is applied, especially leave-one-out learning method has given better performance for the test phase. It is also important that, only approximation coefficients are selected in wavelet analysis after feature selection is applied. Another important result is that, after applying feature selection, features obtained from some faces of marble cubes constitute the majority of all the total selected features. Therefore, correlation of these faces with the direction of minimum pulse wave velocity could be expected. It is seen that nearly half of the selected features are in the direction of 2<sup>nd</sup> and 4<sup>th</sup> faces, and the most of the marble samples have the minimum pulse wave velocity in this direction. The least number of selected features are in the direction of 1<sup>st</sup> and 3<sup>rd</sup> faces, and again, the least number of marble samples have minimum pulse wave velocity in this direction. Nevertheless, more investigation is needed to reach certain conclusions about the correlation between the faces with selected features and direction of minimum pulse wave velocity values.

Finally, we have to remember that inner structure of cubic marble samples are not known to us, although this inner structure greatly affects and determines the UCS values of marble cubes. Therefore, in the future, if any method can be developed to receive information about inner structures of marble cubes, better prediction of UCS values could be possible.



## REFERENCES

- Addison, P. S. (2002). *The illustrated wavelet transform handbook: Introduction theory and applications in science, engineering, medicine and finance*. UK: Institute of Physics Publishing.
- Ardalı, E. (2008). *Classification of marble textures using neural networks and image processing methods*, M.Sc. Thesis, Dokuz Eylül Üniversitesi.
- Delgado, J. D. L., Alajarin, J. M., & Balibrea, L. M. T. (2003). Classification of marble surfaces using wavelets. *Electronics Letters*, vol. 39 (9), 714 – 715.
- Gokceoglu, C. (2002). A fuzzy triangular chart to predict the uniaxial compressive strength of the Ankara agglomerates from their petrographic composition. *Engineering Geology*, vol. 66 (1-2), October 2002, 39-51.
- Gutierrez-Osuna, R. (2008a). *Feature subset selection*. Retrieved April 8, 2011, from [http://courses.cs.tamu.edu/rgutier/cpsc689\\_f08/l11.pdf](http://courses.cs.tamu.edu/rgutier/cpsc689_f08/l11.pdf)
- Gutierrez-Osuna, R. (2008b). *Cross-validation*. Retrieved April 8, 2011, from [http://courses.cs.tamu.edu/rgutier/cpsc689\\_f08/l13.pdf](http://courses.cs.tamu.edu/rgutier/cpsc689_f08/l13.pdf)
- Haykin, S. (1999). *Neural networks: A comprehensive foundation* (2nd ed.). NJ: Prentice Hall.
- MATLAB Image Processing Toolbox, R2011a Documentation. (2011). *Regionprops*. Retrieved June 9, 2011, from <http://www.mathworks.com/help/toolbox/images/ref/regionprops.html>
- Otsu, N. (1979). A threshold selection method from gray-level histograms. *Systems, Man and Cybernetics, IEEE Transactions on*, vol. 9 (1), 62-66.
- Önal, O. (2008). *Digital image processing techniques for analyzing sectional characteristics of some geomaterials*, Ph.D. Thesis, Dokuz Eylül Üniversitesi.
- Selver, M. A., Ardalı, E., Onal, O., & Akay, O. (2008). Predicting uniaxial compressive strengths of brecciated rock specimens using neural networks and

different learning models. *23rd International Symposium on Computer and Information Sciences, 2008, ISCIS '08, 27-29 Oct. 2008*, Page(s): 1-4.

Sonmez, H., Tuncay, E., & Gokceoglu, C. (2004). Models to predict the uniaxial compressive strength and the modulus of elasticity for Ankara Agglomerate. *International Journal of Rock Mechanics and Mining Sciences*, vol. 41 (5), July 2004, 717-729.

Unser, M. (1986). Sum and difference histograms for texture classification. *IEEE Transactions on Pattern Analysis and Machine Intelligence*, vol. PAMI-8 (1), 118-125.

## LIST OF FIGURES

Figure 1.1 Destructive laboratory testing to determine UCS (TÜBİTAK MAG 104M358).	1
Figure 2.1 A polished $7 \times 7 \times 7$ cm cubic marble sample.	4
Figure 2.2 Marble block before and after polishing. Visual difference is clear.	5
Figure 2.3 Image acquisition system.	5
Figure 2.4 Labels of marble surfaces.	6
Figure 2.5 Marble images from each quality group; (a) Homogenous limestone, (b) Limestone with veins, (c) Images containing grains separated by cohesive matrix, (d) Homogenous cohesive matrix.	7
Figure 3.1 8 pixel neighborhoods for SDH.	9
Figure 3.2 Two example images.	9
Figure 3.3 (a) and (b) 3-level wavelet decomposition.	14
Figure 3.4 Region and bounding box.	15
Figure 3.5 Ellipse.	16
Figure 3.6 Search strategies (Gutierrez-Osuna, 2008a).	20
Figure 4.1 Supervised learning.	23
Figure 4.2 Structure of an MLP with one hidden layer.	24
Figure 4.3 Learning schemes for (a) holdout (b) random sub-sampling (c) K-fold (d) leave-one-out cross validation methods (Gutierrez-Osuna, 2008b).	26
Figure 4.4 Learning scheme for the bootstrap method (Gutierrez-Osuna, 2008b).	27
Figure 6.1 (a) Axial strength versus sample number, (b) max pulse wave velocity ( $m/s$ ) versus sample number, (c) area ratios overall versus sample number, and (d) effective porosity (%) versus sample number.	41

## LIST OF TABLES

Table 3.1 Sum and difference values of example images.....	10
Table 3.2 Statistical features obtained by SDH.....	11
Table 5.1 Performance results (percentage error) of training and test using all 126 SDH features. ....	30
Table 5.2 Performance results of training and test for 9 SDH features obtained after feature selection. ....	31
Table 5.3 Performance results of training and test phases for all 180 wavelet features. ....	32
Table 5.4 Performance results of training and test phases for 3 wavelet features obtained after feature selection.....	33
Table 5.5 Performance results of training and test phases for all 72 region based features. ....	34
Table 5.6 Performance results of training and test phases for 7 remaining region based features after feature selection. ....	35
Table 5.7 Performance results of training and test phases for all 6 features of nondestructive laboratory tests. ....	37
Table 5.8 Performance results of training and test phases for 3 remaining features of nondestructive laboratory tests. ....	38
Table 6.1 Numbers of total extracted and selected features.....	42
Table 6.2 Numbers of marble cubes per direction with minimum pulse wave velocity.....	43